Physics – Uspekhi **57** (4) 377 – 388 (2014)

100th ANNIVERSARY OF THE BIRTH OF Ya B ZELDOVICH

PACS numbers: 97.10.Gz, 97.60.Jd, **97.80.–d**

Radiation-dominated boundary layer between an accretion disc and the surface of a neutron star: theory and observations

M R Gilfanov, R A Sunyaev

DOI: 10.3367/UFNe.0184.201404e.0409

Contents

1. **Introduction** 377
2. **Emission from the boundary layer** 380
3. **Theory of the boundary layer** 383
4. **Observations of boundary layer radiation in galactic X-ray binary systems** 386
5. **Conclusion** 387
References 388

Abstract. Observations of low-mass X-ray binaries in our Galaxy and external galaxies have drawn attention to the accretion disc boundary layer where the accreting matter slows down from its Keplerian orbital velocity of about half of the speed of light to a neutron star's rotational velocity and in which it releases about half of its gravitational energy. Correspondingly, a hot spectral component appears in the emission of accreting neutron stars, which is absent in accreting black holes. We review different approaches to the problem of the radiation-dominated boundary layer. In particular, we consider the theory of a levitating spreading layer, which assumes that the accreting matter slows down while spreading over the neutron star surface.

1. Introduction

About half of the known bright X-ray sources in the Milky Way comprise a neutron star with a relatively weak magnetic field, onto which matter accretes from a companion low-mass donor star in the close binary system. X-ray luminosity of these sources is $\sim 10^4 - 10^5$ times higher than the bolometric luminosity of our Sun, and their emission demonstrates strong variability on time scales from several dozen years to a few milliseconds. The necessity of interpreting the results of observations of these sources brought to the attention of astrophysicists the problem of the boundary layer in which the accreting matter decelerates from the Keplerian rotational velocity to the neutron star rotational velocity. About half the gravitational energy of accreting matter is released in this process, providing around half the observed luminosity in sources like Scorpio X-1. The important role of the boundary layer is not only due to its high energy release, but also because of its relatively low surface area comparable to or less than the neutron star surface. As a result, a luminous hot spectral component arises in spectra of accreting neutron stars, which is absent in the emission from accreting black holes.

In this review, we discuss different theoretical approaches to solving the boundary layer problem. In particular, we focus on the theory of a spreading layer, in which the deceleration of matter occurs simultaneously with its distribution over the neutron star surface. The spreading layer model changed the classical concept in which the boundary layer was considered as an extension of the accretion disk, whereas meridional motion of matter and radial energy transfer were neglected. The model of such a layer was proposed by Inogamov and Sunyaev [1] in 1999 in the 'shallow water' approximation. It turned out to be successful, both in theoretically describing the matter deceleration process and accreting matter redistribution over the neutron star surface and in interpreting observational results.

The key to the spreading layer theory lies with the problem of deceleration of a hypersonic flow moving above the neutron star surface with a velocity of $\sim 1/2$ of the velocity of light c. Imagine a neutron star with a weak magnetic field — a carefully polished billiard ball with a mass of one and a half solar masses ($M_\odot \approx 2 \times 10^{33}$ g) and a radius of $\sim 10-15$ km, onto which disk accretion of matter with a high specific angular momentum takes place [2] (Figs 1, 2). The rate of mass transfer from the companion normal star ranges from $\sim 10^{-10} M_\odot$ to $\sim 10^{-8} M_\odot$ per year, or, equivalently, from $\sim 10^{16}$ to 10^{18} g s^{-1}.

At high luminosities, which are typical for accreting neutron stars in close binary systems, the plasma in the levitating boundary layer turns out to be radiation-dominated, i.e., the radiation pressure $P_r = E_r/3$ exceeds the plasma thermal pressure $P_{pl} = 2N_e k_B T_e$, and the velocity of sound there can be as high as $\sim 0.1c$. The X-ray flux density emerging in the spreading layer can be such that the radiation

M R Gilfanov, R A Sunyaev Space Research Institute,
Russian Academy of Sciences,
ul. Profsoyuznaya 84/32, 117997 Moscow, Russian Federation
E-mail: gilfanov@iki.rssi.ru
Max-Planck-Institut für Astrophysik,
Karl-Schwarzschild-Str. 1, 85748 Garching, Germany

Received 17 January 2014, revised 24 February 2014
Uspekhi Fizicheskikh Nauk **184** (4) 409 – 422 (2014)
DOI: 10.3367/UFNr.0184.201404e.0409
Translated by K A Postnov; edited by A Radzig

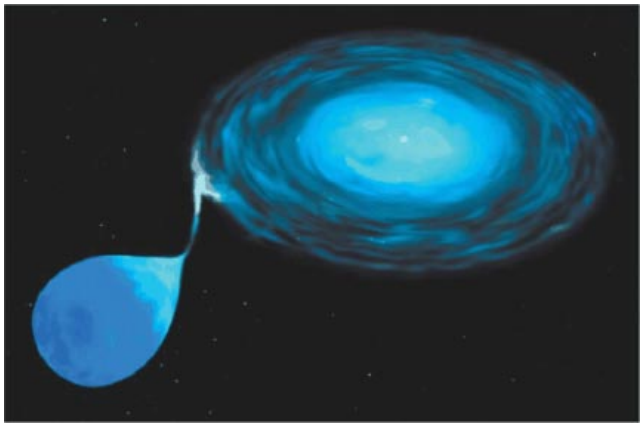

Figure 1. Schematic image of a low-mass X-ray binary system. Shown to the left is the low-mass donor star filling its Roche lobe. The matter from the donor star flows through the inner (first) Lagrangian point and accretes onto the neutron star. Due to the joint action of the gravitational attraction force to the compact object and the centrifugal force, the form of the donor star is strongly nonspherical. The high specific angular momentum of the accreting matter causes the accretion disk to be formed, which fills a significant fraction of the Roche lobe of the compact star residing in its center. (Figure taken from the site http://chandra.harvard.edu.)

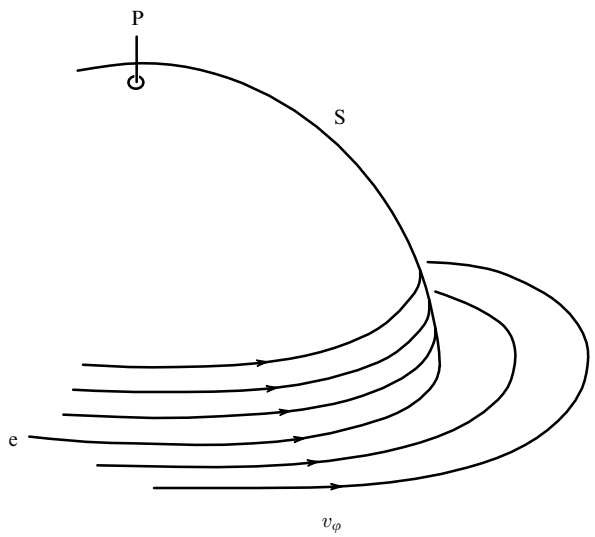

Figure 2. Rotation of matter in the disk and on the neutron star surface: S — neutron star surface, P — neutron star pole, and e — equator. (Taken from [1].)

pressure force balances the difference between the gravitational and centrifugal forces, and the height of the homogeneous atmosphere reaches approximately 1 km. This problem has no analogues in Earth's atmosphere and cannot be modelled in the laboratory. It is one of the most beautiful but still unsolved problems of modern astrophysics.

It is worth mentioning here that in 1969 Zeldovich and Shakura [3] were the first to consider in detail the physical processes that take place in decelerating the radial flow of protons and electrons falling onto the neutron star surface with a weak magnetic field in the context of spherically symmetric accretion. In paper [3], using the solution to the Kompaneets equation [4] found by Zeldovich and Sunyaev [5], its authors first stressed the enormous role of the Comptonization in the formation of the X-ray emission spectrum.

In the Newtonian approximation, half of the gravitational energy released in accretion, namely

$$L_{\rm d} = \frac{1}{2}\,\dot{M}\,\frac{GM_*}{R_*}\,, \tag{1}$$

is emitted in an extended disk (G is the Newtonian constant of gravitation, M_* and R_* are the mass and radius of the neutron star, respectively). The other half of the energy is contained in the rotational kinetic energy of matter at the inner disk boundary. The matter in the accretion disk rotates with the Keplerian velocity $v_{\rm K} = (GM/R_*)^{1/2}$, which can reach half the velocity of light near the neutron star surface. The observed neutron star spin frequencies in low-mass X-ray binaries fall in the range of $\sim 45-600$ Hz [6], which corresponds to the velocities of motion of the neutron star surface of the order of $(0.01-0.2)\,c$. The problem of decelerating the weakly relativistic flow of a collisional plasma in a thin boundary layer arises, in which the rotational velocity of matter decreases from half the velocity of light to the rotational velocity of the stellar surface at the equator, and where all the excessive rotational kinetic energy dissipates (Figs 2, 3). The angular momentum of the accreting matter must be transferred to the star, thus accelerating its rotation (which, apparently, explains the large dispersion in the observed neutron star spin frequencies [6]). Taking into account that part of the energy is spent on the neutron star spin-up, the luminosity of the boundary layer is defined by the following formula

$$L_{\rm BL} = \frac{1}{2}\,\dot{M}\,\frac{GM_*}{R_*}\left(1-\frac{\Omega_*}{\Omega_{\rm K}}\right)^2, \tag{2}$$

where Ω_* is the rotational frequency of a neutron star, and $\Omega_{\rm K}$ is the Keplerian frequency at its surface [7–9]. As $\Omega_{\rm K} \sim 1.5-2$ kHz, for a typical neutron star the term in the parentheses in formula (2) is close to unity, i.e., the other half of the gravitational energy of the accreting matter is released in the boundary layer near the neutron star surface.

In astrophysics, one frequently uses the notion of the Eddington luminosity:

$$L_{\rm Edd} = \frac{4\pi GMm_{\rm p}c}{\sigma_{\rm T}} \approx 1.3\times 10^{38}\,\frac{M_*}{M_\odot}\ {\rm erg\ s^{-1}}\,. \tag{3}$$

It is straightforward to derive the Eddington luminosity as follows. Consider a proton and electron pair in the gravitational field of an object with mass M_* and luminosity L [erg s^{-1}]. The attractive gravitational force acting on the proton from the star (compact object), $F_{\rm grav} = GM_*m_{\rm p}/r^2$, is balanced by the radiation pressure acting on the electron, $F_{\rm lp} = \sigma_{\rm T}q/c$, where $q = L/4\pi r^2$ is the radiation flux from an isotropically radiating source at distance r, and $\sigma_{\rm T} = 8\pi r_{\rm e}^2/3$ is the Thomson scattering cross section (the plasma near a bright X-ray source is strongly ionized and its temperature is very high, so the Thomson scattering is the main contributor to matter opacity). The spherically symmetric accretion is possible only if $F_{\rm grav} > F_{\rm lp}$. For $F_{\rm grav} < F_{\rm lp}$, plasma outflow from the radiation source should begin. These two forces are balanced at the Eddington luminosity determined by relation (3). Remarkably, the brightest X-ray sources in binary stellar systems in our Galaxy and other galaxies show luminosities at the level of Eddington luminosity for the neutron star [10]. This is a huge luminosity, which is 30,000 times as high as the

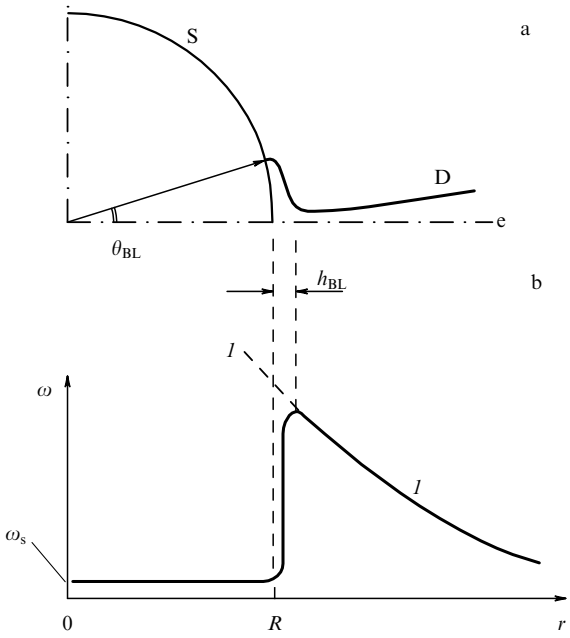

Figure 3. Boundary layer between the accretion disk and neutron star surface. (a) The geometry of the classical model at relatively low accretion rates, $\dot{M} \sim 0.1\dot{M}_{\rm Edd}$: e — equatorial plane, D — accretion disk, S — neutron star surface. (b) The angular velocity ω as a function of radial coordinate r: *1* — Keplerian rotation, $\omega \propto r^{-3/2}$, $h_{\rm BL}$ and $\theta_{\rm BL}$ — radial and meridional boundary layer sizes, respectively. The neutron star is assumed to rigidly rotate with angular velocity $\omega_{\rm s}$. (Taken from paper [1].)

bolometric luminosity of our Sun. Below, we shall also use the critical Eddington radiation flux from the unit neutron star surface:

$$q_{\rm Edd} = \frac{L_{\rm Edd}}{4\pi R_*^2} = \frac{GM_* m_{\rm p} c}{R_*^2 \sigma_{\rm T}} = 10^{25}\,\frac{M_*}{M_\odot}\left(\frac{10\ {\rm km}}{R_*}\right)^2 {\rm erg\ s^{-1}\,cm^{-2}}\,. \tag{4}$$

Such a significant flux of thermal radiation, which is comparable to the radiation flux from a powerful laser, can be emitted only when the surface has a temperature higher than $\sim 2 \times 10^7$ K, or ~ 2 keV. (This estimation was made using the Stefan–Boltzmann formula under the simplest assumption of a black-body emitting surface.) At such temperatures, the peak of emission falls into the X-ray range. It should be emphasized that for the critical Eddington radiation flux the radiation pressure is balanced by the attractive gravitational force of the star, and the matter in such a radiation field can levitate.

Apparently, around a half of about 300 known X-ray sources in stellar binary systems in our Galaxy represent accreting neutron stars with relatively weak magnetic fields ($< 10^8$ G) [10–12]. Several hundred such sources are being observed by Chandra and XMM-Newton (the X-ray Multi-Mirror Mission-Newton) in external galaxies, where their number is proportional to the host galaxy mass: for each $10^{11} M_\odot$ stars there are about 10^2 systems with luminosity above $\sim 0.1 L_{\rm Edd}$ [13]. The accretion of matter with the Keplerian angular momentum in these systems can spin up the neutron star rotation to millisecond periods. It is believed that this process is responsible for the appearance of millisecond pulsars after the accretion has stopped [14–16].

The pressure of a magnetic field with the strength below $\sim 10^8$ G cannot significantly affect the accretion flow dynamics. In the certain range of luminosities (i.e., accretion rates), these neutron stars can appear as X-ray bursters. In X-ray bursters, in the matter that was accreted onto the neutron star surface, mostly composed of hydrogen and helium, quasiperiodically, every few hours, days, or weeks, the explosive burning of helium occurs, leading to synthesis of carbon, oxygen, and heavier elements [17]. Observations of these bright X-ray bursts with a duration of about 10 seconds have also confirmed that the nuclear burning flame propagates across the entire neutron star surface, which is possible only if the magnetic field is relatively weak.

Notice that black holes have no solid surfaces on which accreted matter can accumulate and compress up to densities and temperatures which are needed for a nuclear explosion to occur. Therefore, observations of X-ray bursts from accreting objects prove their neutron star nature [18].

Thus, around 100 bright X-ray sources in our Galaxy are neutron stars with low surface magnetic fields in close binary systems accreting matter from a low-mass companion normal star or white dwarf. These sources are called low-mass X-ray binaries (see Fig. 1). It is in these systems that most of the X-ray emission comes from the radiation-dominated levitating boundary layer residing close to the neutron star surface. The observed emission brings information about the boundary layer parameters and instabilities developed inside it and leading to the observed rapid variability of the emerging radiation flux.

Low-mass X-ray binaries demonstrate strong aperiodic and quasiperiodic variability of X-ray emission in the wide frequency range with characteristic rms (root-mean-square) amplitudes up to several dozen percent [19], which is due to turbulence emerging in the accretion disk and phenomena occurring on the interface between the accretion disk and neutron star surface. The presence of relatively narrow peaks in the power spectrum — so-called quasiperiodic oscillations (QPOs) [20, 21] — suggests the presence of resonances in the accretion flow (for example, related to the beats between the Keplerian frequency at the inner accretion disk edge and the neutron star spin frequency), the origin and nature of which are not completely clear so far.

The discovery by the RXTE (Rossi X-ray Timing Explorer) orbital observatory of kilohertz QPOs with frequencies of around 1 kHz [21] was remarkable but expected. As a rule, two QPO peaks are observed, and their frequencies can vary from observation to observation, but the frequency difference between them remains approximately constant. Apparently, these oscillations are related to the presence of inhomogeneities in the accretion disk near its inner boundary. Their frequencies may correspond to fundamental frequencies of particle motion in the strong gravitational field close to the neutron star: the Keplerian frequency, and the precession frequency of the periastron of slightly eccentric orbits [22].

It may be now regarded as proven that the modulation of X-ray emission leading to the phenomena of aperiodic and quasiperiodic variability at frequencies $\nu \geqslant 10^{-2} - 10^{-1}$ Hz occurs near the neutron star surface, in the boundary layer, and at the inner edge of the accretion disk [23, 24]. At the same time, variability at lower frequencies is produced in the extended accretion disk and modulates the mass accretion rate with which matter enters the boundary layer, which, naturally, is reflected in its luminosity [23, 25].

We note that this review is only focused on accreting neutron stars with high luminosity ($\gtrsim 10^{-2} L_{\rm Edd}$). In neutron stars with smaller luminosities, the role of radiation pressure is lower, and the deceleration of accretion flow near the neutron star surface can occur in a totally different way. Nor do we consider neutron stars with a strong magnetic field of $B \sim 10^{11} - 10^{12}$ G. X-ray sources with such neutron stars — X-ray pulsars — are, typically, associated with young systems, high-mass X-ray binaries, which are found in the regions of intense star formation [13]. The strong magnetic field of a young neutron star destroys the accretion disk at large distances from its surface and radically changes the structure of the accretion flow. In these sources, collimation of the flow by a magnetic field leads to the appearance of X-ray pulsations [26–31].

2. Emission from the boundary layer

Analysis in the framework of general relativity (GR) shows that the fraction of energy released near the surface of a nonrotating neutron star can be significantly higher than the Newtonian value determined by equation (2). For example, the luminosity of the boundary layer in the Schwarzschild metric is two times as high as that of the accretion disk, if the neutron star radius exceeds that of the innermost stable circular Keplerian orbit [32]:

$$R_{\rm ISCO} = 3R_{\rm S} = \frac{6GM_*}{c^2} \approx 8.86\,\frac{M_*}{M_\odot}\ \text{km}\,, \tag{5}$$

where $R_{\rm S} = 2GM_*/c^2$ is the Schwarzschild radius. The fraction of the boundary layer luminosity can be even higher if $R_* \leqslant R_{\rm ISCO}$ (Fig. 4). However, a 'gap' opens up in this case

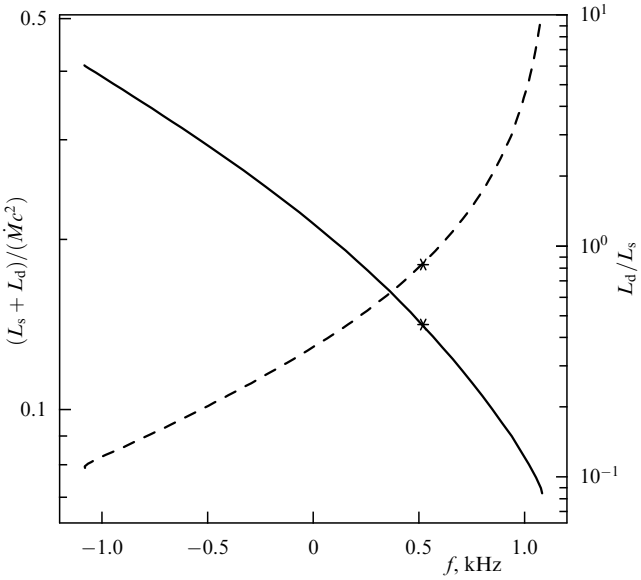

Figure 4. Total energy release $L_{\rm d} + L_{\rm s}$ in the accretion disk and on the neutron star surface (solid curve) and their ratio $L_{\rm d}/L_{\rm s}$ (dashed curve) as a function of the neutron star spin frequency f. Calculations were done for the constant neutron star gravitational mass $M = 1.4M_\odot$ and moderately stiff equation of state (EOS FPS, by Friedman–Pandharipande–Skyrme) [33]. Asterisks in the curves show the frequency f_* at which the neutron star radius is equal to the innermost stable circular Keplerian orbit radius. For lower neutron star frequencies, $f \leqslant f_*$, a gap between the inner edge of the accretion disk and the neutron star surface appears. (Taken from paper [34].)

between the inner edge of the accretion disk and the neutron star surface, inside which the matter moves along a loosely wound spiral trajectory with a velocity approaching the radial free-fall velocity ($\sim 0.5c$) and is decelerated when colliding with the neutron star surface. Clearly, the structure of the flow under these conditions will be different from that in the classical problem of boundary layer. The matter braking in the collision with the neutron star surface and emerging radiation were considered in paper [35]. The neutron star radius with a high probability lies within the range of $\sim 10-15$ km [24, 36, 37], i.e., it measures $\sim (2.5-4)\,R_{\rm S}$. So, up to now it is unclear whether the configuration with a gap between the accretion disk and the neutron star is realized in nature. On the other hand, as was demonstrated in paper [35], the gap should lead to the appearance of hard power-law emission spectra in the energy range up to ~ 200 keV. This seems to contradict observational data (see Section 4) and may suggest that there is a gap between the accretion disk and neutron star, at least in the majority of the X-ray binaries in the Milky Way. Note that the gap can be absent for $R_* \leqslant R_{\rm ISCO}$, too, if the effective thickness of the boundary layer in the equatorial region of the star exceeds the gap size.

The dependences of the total energy release on the spin frequency and the ratio of contributions from the accretion disk and boundary layer around a neutron star with gravitational mass $1.4M_\odot$ are presented in Fig. 4. Shown are the results of accurate GR calculations in the realistic spacetime metric and plausible equation of state in the neutron star core [9, 34]. The positive and negative values of the neutron star spin frequency f correspond to co- and counter rotations of the star and inner accretion disk, respectively. As expected, the fraction of energy released in the boundary layer decreases with an increase in the neutron star spin frequency. However, this decrease occurs more rapidly than predicted by the Newtonian formula (2). The inverse behavior is observed when the disk counter-rotates with the neutron star: then, most of the energy is released in the boundary layer. It is also interesting to note that in the situation with the counter-rotating disk and neutron star, the accretion efficiency $\eta = L/\dot{M}c^2$ highly exceeds the Newtonian value and can be as high as $\eta \approx 0.67$ for massive neutron stars [34]. This is due to the neutron star spin-down. For comparison, efficiency of accretion onto a nonrotating $1.4M_\odot$ neutron star is $\eta \approx 0.21$ [34].

For the practical application to the interpretation of observational data, the following approximate formulas for the accretion disk ($L_{\rm d}$) and boundary layer ($L_{\rm s}$) luminosities, derived in Ref. [34], are useful:

$$L_{\rm s} + L_{\rm d} \approx \left(0.213 - 0.153\,\frac{f}{1\,\text{kHz}} + 0.02\left(\frac{f}{1\,\text{kHz}}\right)^2\right)\dot{M}c^2\,, \tag{6}$$

$$\frac{L_{\rm s}}{L_{\rm s} + L_{\rm d}} \approx 0.737 - 0.312\,\frac{f}{1\,\text{kHz}} - 0.19\left(\frac{f}{1\,\text{kHz}}\right)^2. \tag{7}$$

The role of the boundary layer in the formation of the radiation spectra of accreting neutron stars in close binary systems is determined not only by its significant contribution to the luminosity, but also by the fact that the surface area of the boundary layer is much smaller than that of the accretion disk. For this reason, the temperature of emission from the boundary layer is several times as high as that of the accretion

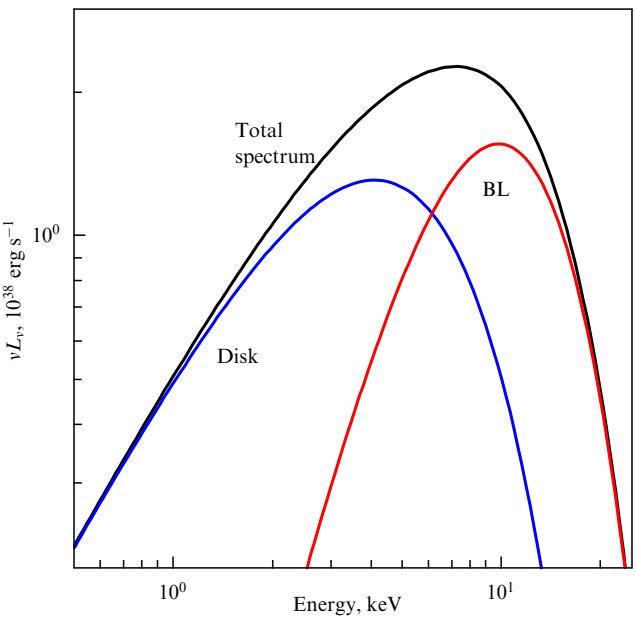

Figure 5. Emission spectrum of an accreting neutron star in a close binary system with luminosity $\sim 2 \times 10^{38}$ erg s^{-1}. Shown are contributions from the accretion disk ('Disk'), the boundary layer ('BL'), and their sum ('Total').

disk:

$$T_{\rm BL} \sim T_{\rm disk} \left(\frac{S_{\rm disk}}{S_{\rm BL}} \right)^{1/4}, \tag{8}$$

where $S_{\rm BL}$ and $S_{\rm disk}$ are the surface areas of the boundary layer and accretion disk inner region, respectively. Different models of the boundary layer predict greatly differing area ratios $S_{\rm disk}/S_{\rm BL}$ (see Section 3). Observations show that at an accretion rate of about 0.5 the Eddington value, the boundary layer temperature is $\sim 3-4$ times as high as that of the accretion disk (see Section 4). The spectrum of the accreting neutron star for such accretion rates is schematically depicted in Fig. 5. At smaller accretion rates, the accretion disk temperature is consequently lower.

The effective temperature of the boundary layer is limited by the value at which the radiation flux becomes equal to the local Eddington value [equation (4)]. If the local energy release exceeds the critical Eddington value (i.e., the radiation pressure is higher than the gravitational attraction), the matter outflow would reduce the accretion rate and, correspondingly, the local energy release to the Eddington value.[1] This broadly known theoretical inference is confirmed by observations: luminosities of the brightest neutron stars in our Galaxy typically do not exceed the Eddington limit calculated taking into account contributions from both the accretion disk and the boundary layer (see below) [10, 23]. By neglecting the centrifugal force, it is easy to show that the Eddington temperature for fully ionized hydrogen is defined by the equation

$$\sigma_{\rm T} \frac{\sigma T_{\rm Edd}^4}{c} = \frac{G M_* m_{\rm p}}{R_*^2} \left(1 - \frac{R_{\rm S}}{R_*} \right)^{3/2}, \tag{9}$$

[1] It is well known that the luminosity of an accreting source can exceed the Eddington limit by some moderate factor in the case of a special geometry of the accretion flow or in the case of intense outflow of matter. Consideration of these special cases lies beyond the scope of this review.

where σ — is the Stefan–Boltzmann constant, and $T_{\rm Edd}$ is the Eddington temperature for an observer at infinity. For the neutron star with a mass of $1.4 M_\odot$ and radius of 10–15 km, formula (9) gives $T_{\rm Edd} \sim 1.5$ keV. Formula (9) takes into account that the gravitational redshift reduces the temperature registered by an observer at infinity. For the typical masses and radii of neutron stars, its effect is $\sim 15\%$.

It should be noted that light ray bending in the strong gravitational field of a rotating neutron star can complicate the geometry of the problem. In particular, the observer can see part of the emission from the second (invisible in the classical approximation) hemisphere of the neutron star. The neutron star rotation ($v/c \sim 0.1$) further distorts the boundary layer emission spectrum (by analogy of the Doppler effect in the classical approximation).

However, the most important effect, which should be taken into account when making comparison with observations, is that, due to Compton scattering on free electrons in the neutron star atmosphere, the color temperature $T_{\rm c}$ of the boundary layer emission (as well as of the accretion disk) differs from its effective temperature $T_{\rm eff}$ — the spectrum turns out to be 'harder' than the Planck spectrum with the same luminosity. For the typical plasma parameters in the accretion disk, one finds $T_{\rm c}/T_{\rm eff} \sim 1.7$ [38], giving the color temperature of ~ 2.5 keV. This is close to the values observed in low-mass X-ray binaries in our Galaxy (see Section 4).

As the neutron star radius is close to that of the innermost stable Keplerian orbit around a nonrotating black hole, $R_{\rm ISCO} = 3R_{\rm S}$, it should be expected that the overall structure of the accretion disk is independent of the nature of the central compact object — a neutron star or black hole. This fact is confirmed by observations. In particular, in the case of accretion onto a neutron star, as in the case of accretion onto a black hole, two spectral states, soft (high) and hard (low), are observed, as illustrated in Fig. 6. The transition from the hard spectral state to the soft state occurs when the luminosity is above a few percent of the Eddington limit (3). The spectrum of the accretion disk around a neutron star or a black hole can be equally fitted by one model (see, for example, Ref. [42]), and the power spectrum of low-frequency X-ray flux fluctuations (which is determined by the properties of the turbulence in the accretion disk) in both classes of sources follows a power law $P_\nu \propto \nu^{-\alpha}$ with exponent $\alpha \approx 1.3$ (Fig. 7).

When making comparisons of emission spectra from accreting neutron stars and black holes, it should be borne in mind that there is no boundary layer in the latter case. Correspondingly, there is no spectral component produced in the boundary layer. It is interesting to note that, for this reason, the luminosity of an accreting neutron star will be 2–3 times as high for the same accretion rate as that of an accreting Schwarzschild black hole. We remind the reader that the accretion efficiency $\eta = L/\dot{M}c^2$ onto a nonrotating black hole is $\eta \approx 0.057$ [32], and onto a neutron star with account for the boundary layer emission it is $\eta \approx 0.21$ [see Fig. 4 and equation (7)] [34]. In the case of an accreting black hole, the 'missing' energy, which is stored in the form of the kinetic energy of accreting matter, is advected beyond the black hole event horizon. In contrast, this energy is released in the boundary layer near the neutron star surface in the case of an accreting neutron star. Another interesting consequence is that the specific critical luminosity $L_{\rm crit}/M_*$, at which the

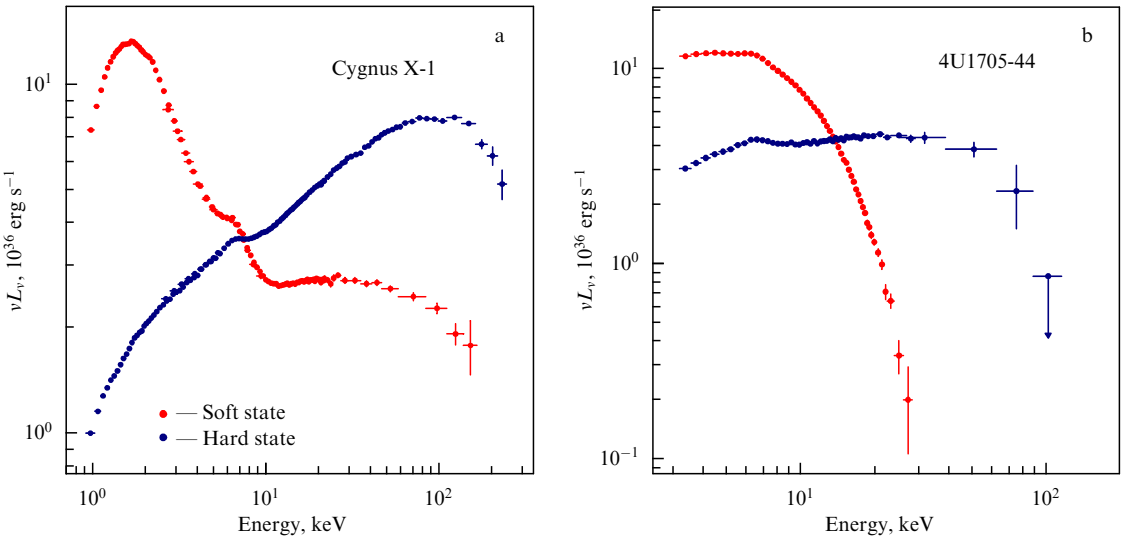

Figure 6. Observed spectral energy density in the soft and hard spectral states of the black hole Cygnus X-1 (a), and of the neutron star 4U 1705-44 (b). In both cases, the radical change in the shape of emission spectra is related to the redistribution of the fractions of energy emitted in the optically thick accretion disk and optically thin hot corona located in the immediate vicinity of the compact object. In the case of neutron stars, the transition of the accretion disk and boundary layer from the optically thick regime to the optically thin regime occurs simultaneously. In the high state, the neutron star spectrum has higher color temperature than the black hole spectrum, due to the boundary layer contribution and smaller emitting area because of the smaller linear size of the neutron star. The appearance of power-law spectral components with exponential cut-off is characteristic of Comptonization of low-frequency radiation in hot plasma. The spectral slope is determined by the temperature of electrons and by the mean number of scatterings in the hot plasma cloud (or, equivalently, by the optical depth) [39]. In the hard state, the spectrum of the Comptonized emission from a neutron star is softer than from a black hole. This is due to the emission of the neutron star surface which cools electrons in the corona [40]. The spectral density is given in units of νL_ν, which characterizes the luminosity in the spectral energy range ΔE of order E. (Taken from papers [41, 42].)

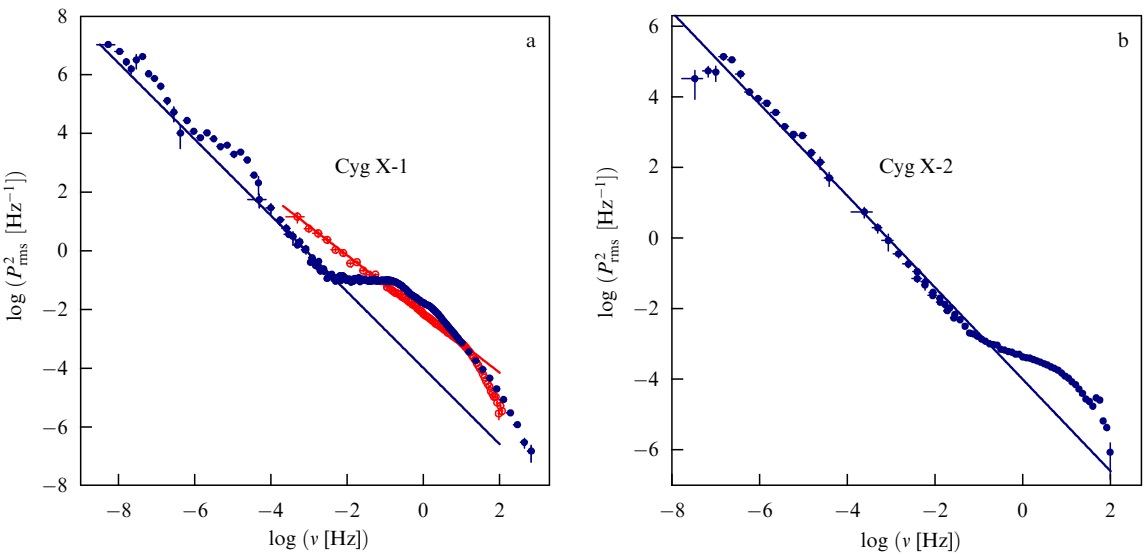

Figure 7. Broad band power spectra of X-ray fluctuations from (a) black hole Cygnus X-1, and (b) neutron star Cygnus X-2 (dark symbols). Solid lines show the power law $P_\nu \propto \nu^{-1.3}$ with the same normalization in both figures. The low-frequency part of the power spectrum, $\log \nu \leqslant -2$, which can be well fitted by the power law, is due to turbulence and instabilities in the extended accretion disk. The additional component of aperiodic variability at frequencies $\log \nu \geqslant -2$ can be generated in the optically thin corona near the black hole, $r \leqslant 100 R_{\rm S}$ (Cygnus X-1) [43], or in the boundary layer and at its interface with the accretion disk (neutron star in Cygnus X-2) [23]. Notice that the mass of the black hole in Cygnus X-1, which is $\approx 15 M_\odot$ [44], is about 10 times as high as the typical neutron star masses. As the characteristic times of most of the instabilities in the accretion disk increase with the compact object mass [45], i.e., $\nu \propto 1/M_*$, in Cygnus X-2 this aperiodic variability component is observed at higher frequencies. Light symbols in the left panel show this power spectrum of the black hole Cygnus X-1 in the high state and its approximation by the power law $P_\nu \propto \nu^{-1}$. In this case, the optically thick and geometrically thin accretion disk likely extends to the innermost stable Keplerian orbit, and the optically thin quasispherical part of the accretion flow is insignificant. (Taken from paper [42].)

radiation pressure can lead to a substantial outflow of the accreting matter, for neutron stars is $\sim 2-3$ times as high as that for black holes. It is important to stress that the emission of the spreading layer weakly affects matter of the accretion disk and its radial motion.

In spite of the similar global structure of accretion flows around neutron stars and black holes, the presence of a neutron star with a solid surface, at which the kinetic energy of the accreting matter is released and which can emit photons, leads to several differences between accreting

neutron stars and black holes. The most obvious difference is that, in the case of neutron stars, the low-temperature (in comparison with the temperature of electrons in the hot corona, $T_e \sim 50-100$ keV) emission of the neutron star surface leads to a more effective cooling of the corona and a decrease in the Comptonization parameter [40]. For this reason, power-law spectra from neutron stars in the hard state demonstrate steeper slopes and thermal cut-off at lower energies than do black holes (see Fig. 6).

At low accretion rates in inner region of the accretion disk, the transition to the advection-dominated radiation-inefficient regime of accretion becomes possible [46]. In this regime, plasma in the accretion disk becomes two-temperature: protons have a temperature of several dozen MeV, while electrons only up to 100 keV. However, during accretion onto a neutron star, the advected energy, unlike in accretion onto a black hole, cannot completely disappear in the black hole and must be radiated in the boundary layer near the neutron star surface [47]. Already at luminosities exceeding approximately several percent of the Eddington limit, the emission from the boundary layer will be sufficient to cool the accretion flow [40] due to Comptonization [4, 48]. The advective solution with supercritical accretion and a geometrically thick disk [49, 50] is also inapplicable to accretion onto neutron stars, where there is no black hole and where radiation generated during accretion, but locked in the optically thick accretion flow, can be advected. Neutron stars have the surface, while in a steady state all the energy released during accretion should escape to infinity.

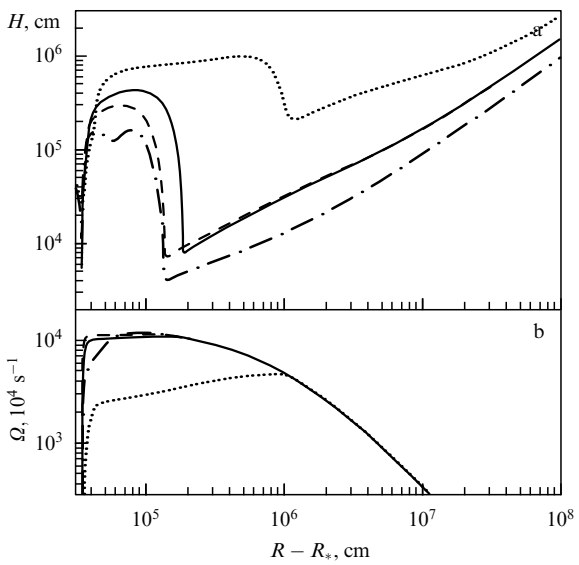

Figure 8. Vertical accretion disk thickness H (a) and the angular velocity of rotation of matter Ω (b) as functions of the distance to the neutron star surface. Shown are the results for different accretion rates onto a non-rotating neutron star: $\dot{M} = 10^{-10} M_\odot\,\mathrm{yr}^{-1}$ (dashed-dotted line), $\dot{M} = 10^{-9} M_\odot\,\mathrm{yr}^{-1}$ (dashed line), and $\dot{M} = 10^{-8} M_\odot\,\mathrm{yr}^{-1}$ (solid line). Also shown is the result of calculations for a neutron star with spin frequency $f_* = 636$ Hz, accreting at a rate of $\dot{M} = 10^{-9} M_\odot\,\mathrm{yr}^{-1}$ (dashed curve). Note the small disk thickness in the transition zone from accretion disk to boundary layer, as well as sharp growth of the accretion flow thickness in the boundary layer. At high accretion rates, $\dot{M} \to \dot{M}_{\mathrm{Edd}}$, the radial and vertical sizes of the boundary layer become comparable to the neutron star radius. Calculations were done for the standard α-model of the turbulent viscosity [2] for $\alpha = 0.1$. (Taken from paper [57].)

3. Theory of the boundary layer

The classical model of the boundary layer developed in 1970s–1980s [7, 51–56] treats the boundary layer as a part of the accretion disk. This means that the motion of matter in the direction perpendicular to the accretion disk plane is neglected ($v_z \ll v_R$), as well as the radial radiation transfer. (Note that in more recent papers this assumption was lifted (see, for example, Ref. [56].) In this model, the deceleration of matter in the boundary layer is due to turbulent or magnetic viscosity, much like in the accretion disk. The turbulent viscosity is assumed to be effective enough for the matter deceleration to occur in the course of a finite number of Keplerian revolutions, similar to deceleration of a satellite entering Earth's atmosphere. The angular velocity derivative with respect to the radial coordinate in the boundary layer is positive, $\mathrm{d}\omega/\mathrm{d}r > 0$ (see Fig. 3). By neglecting the radiation pressure and matter spreading over the neutron star surface, we can calculate the characteristic thickness of the boundary layer: as in the accretion disk, it is determined by the scale height of the isothermal atmosphere, taking into account the tangential projection of the gravitational attractive force:

$$H_{\mathrm{BL}} \approx \sqrt{2} R_* \frac{c_{\mathrm{s}}}{v_{\mathrm{K}}}\,, \tag{10}$$

and the radial extension of the boundary layer is defined by the height of the isothermal atmosphere in the radial direction:

$$\Delta R_{\mathrm{BL}} \approx R_* \frac{c_{\mathrm{s}}^2}{v_{\mathrm{K}}^2 (1 - \Omega_*^2/\Omega_{\mathrm{K}}^2)}\,, \tag{11}$$

where c_{s} is the velocity of sound, and v_{K} is the Keplerian velocity near the neutron star surface [7]. The factor in parentheses on the right-hand side of equation (11) takes into account the centrifugal force effect counter-acting gravitational attraction from the neutron star. As the velocity of sound in the radiation-dominated boundary layer is high, its radial size and vertical thickness turn out to be comparable. The boundary layer structure, obtained in detailed numerical simulations in paper [57] in the classical approximation, is demonstrated in Fig. 8.

An interesting prediction of the accretion disk theory is the formation of a narrow (in height) 'neck' (it is clearly visible in Fig. 8) near the inner disk edge. From outside of the neck, viscous stresses transfer the angular momentum outward. Turbulent friction leads to energy dissipation and heating of the disk matter. The rotational velocity gradient changes sign closer to the neutron star surface, and viscous stresses transfer the angular momentum toward the star. In the neck region, the viscous stresses are small; equally small are the matter heating and pressure, as well as radiation pressure. This is the reason for the neck formation. Figure 8 shows that at sufficiently low accretion rates the theory and numerical calculations predict a neck thickness as small as a few hundredths of the stellar radius. Here, the neck is thinner than the disk thickness at distances of a few stellar radii. For high accretion rates, $\dot{M} \to \dot{M}_{\mathrm{Edd}}$, the radiation transfer in the radial direction and advection of radiation in the disk become important. This noticeably increases the neck thickness.

In the numerical solution of the classical boundary layer problem found in paper [57], the boundary layer size is a fraction of the neutron star radius, and at a sufficiently high accretion rate becomes comparable to the stellar radius (see Fig. 8). This is related to the fact that the radiation flux from unit surface of the boundary layer is limited by the local Eddington value [see equation (4)]. The need to radiate the

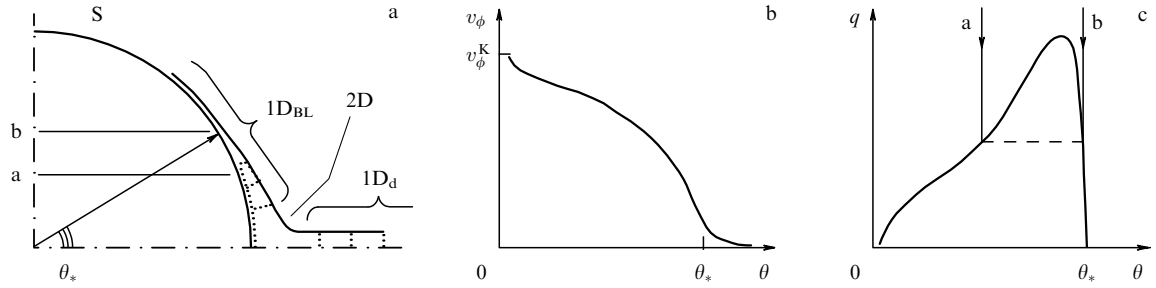

Figure 9. Spreading layer model. (a) Geometry of the spreading layer: S — neutron star surface; $1D_d$ and $1D_{bl}$ — accretion disk and spreading layer on the neutron star surface, amenable to 1D treatment, respectively; 2D — transition zone in which both radial and meridional motions should be taken into account. (b) The linear rotation velocity v_ϕ as a function of the latitude θ. Matter rotation is significant in the latitude range $0 < \theta < \theta_*$; outside this region, the matter loses almost all its azimuthal velocity v_ϕ and barely rotates. (c) The local radiation flux density as a function of latitude θ. Arrows (a) and (b) mark the boundaries of the bright ring on the stellar surface with enhanced energy release. (Takes from paper [1].)

luminosity $L_{BL} \sim 10^{37} - 10^{38}$ erg s^{-1} leads to boundary layer 'inflation' by the radiation pressure, i.e., to an increase in its surface area. Hence, this violates the main assumption underlying the classical boundary layer theory about the insignificantly small role of motions in the direction perpendicular to the accretion disk plane and the total absence of the radiation transfer in the radial direction. This shortcoming of the classical theory was removed in the new theory of the boundary layer developed in the late 1990s [1, 58].

A fundamentally new approach to the boundary layer problem was proposed in paper [1]. Unlike the classical model, the Inogamov–Sunyaev model takes into account both deceleration of the accreting matter and its simultaneous redistribution over the neutron star surface. In this formulation of the problem, it is more appropriate to speak not about the boundary layer between the accretion disk and neutron star, but about the spreading layer of the accreting matter over the neutron star surface (Fig. 9).

Unlike the standard model where the energy release is concentrated near the equator, in the Inogamov-Sunyaev model the energy is released in a sufficiently broad belt on the neutron star surface with meridional size θ_*, which increases with accretion rate. As $\dot{M} \to \dot{M}_{Edd}$, $\theta_* \to 90°$, i.e., at high luminosities, the layer of the rotating matter tends to cover the entire surface of the star. Unlike in the standard model, deceleration of matter in the spreading layer at high luminosities occurs slowly: as the matter decelerates, it makes $\sim 10^2 - 10^3$ revolutions while moving toward the neutron star poles. Motion of matter in the radial direction is determined by the balance between the gravitational force, the projection of the centrifugal force, and the radiation pressure. Due to the high rotational velocity of matter near the equatorial plane, the centrifugal force almost compensates the gravitational acceleration, so the effective value of the local Eddington flux q_{eff} near the equator is much lower than the standard value q_0 determined by equation (9). As the matter decelerates and climbs up toward the poles, the role of the centrifugal force diminishes and $q_{eff}(\theta) \to q_0$. Calculations performed in Ref. [1] showed that in a large part of the spreading layer the radiation flux is equal, with a high accuracy, to the effective local Eddington value: $q(\theta) \approx q_{eff}(\theta)$. Using this result, the meridional size of the spreading layer can be estimated from the following equation

$$\dot{M}\,\frac{(v_\phi^K)^2}{4} = 2\pi R_*^2 \int_0^{\theta_*} q_{eff}(\theta)\,\mathrm{d}\sin\theta\,, \tag{12}$$

where the effective local Eddington flux is given by

$$q_{eff}(\theta) = \frac{m_p c}{R_* \sigma_T}\left[\left(v_\phi^K\right)^2 - v_\phi^2(\theta)\right]. \tag{13}$$

Here, v_ϕ^K is the Keplerian velocity on the neutron star surface. To find θ_* from equation (12), the latitudinal dependence of the rotational velocity, $v_\phi(\theta)$, must be known, which is determined by solving the full problem of matter deceleration in the spreading layer. By neglecting the centrifugal force, one can find the lower limit for θ_*:

$$\theta_* > \arcsin\frac{L_{BL}}{L_{Edd}}\,. \tag{14}$$

Because the angular velocity of matter rotation, $v_\phi(\theta)$, decreases with increasing latitude, equation (13) implies that the local radiation flux increases with latitude to reach a maximum value near the outer boundary of the spreading layer θ_*. This leads to the appearance of two bright belts on the spreading layer (in the northern and southern hemispheres), in which up to $\sim 70\%$ of its total luminosity is radiated (Fig. 9). The enhanced brightness in these belts is due to mechanical advection of thermal energy from the near-equatorial region by the meridional motion of matter (Fig. 10). With increasing accretion rate, the location of the bright belts is shifted toward the rotational poles of the neutron star, and the width of the belts increases (Fig. 11) [1].

As the radiation pressure and the centrifugal force almost adequately compensate for the gravitational attractive force, the effective scale height of the isothermal atmosphere approaches ≈ 1 km, which is much higher than the standard scale height of the isothermal atmosphere of the neutron star in the absence of rotation and radiation pressure which is of order $10 - 100$ cm. As a result, the spreading layer levitates above the neutron star surface. The meridional component of the centrifugal force, directed toward the neutron star equator, determines the spreading layer meridional structure. The propagation of matter in this direction is possible only when the angular momentum is being lost, which leads to a decrease in the meridional component of the centrifugal force [1, 58].

Identifying the deceleration mechanism is the major challenge in the spreading layer problem. The hypersonic flow moving with a velocity of $\sim (0.4 - 0.5)\,c$ above the 'sole' of the spreading layer — the dense atmosphere made of

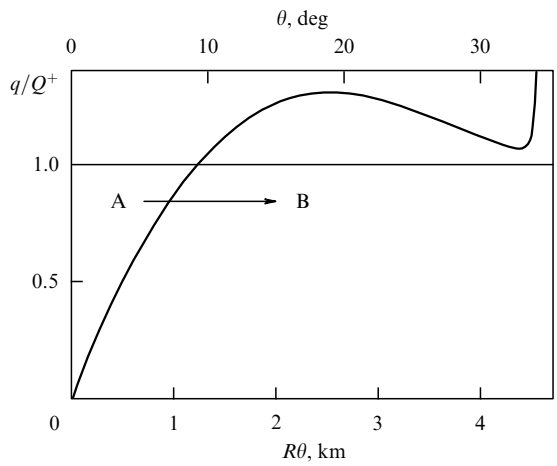

Figure 10. Ratio of energy flux q emitted by the spreading layer unit area to energy release due to friction forces Q^+ per unit contact surface area between the spreading layer and neutron star. Shown is the result of numerical calculations for $L_s/L_{\rm Edd} = 0.2$. θ is the latitude measured from the neutron star equator, $R\theta$ is the linear coordinate along a meridian. Energy is transferred from zone A to zone B due to mechanical advection of thermal energy in the meridional direction, which largely governs the spreading layer dynamics. The energy release in the equatorial plane must vanish; otherwise, the radiation pressure pushes away the accretion disk in which the gravitational attraction is balanced by the centrifugal force. (Taken from paper [1].)

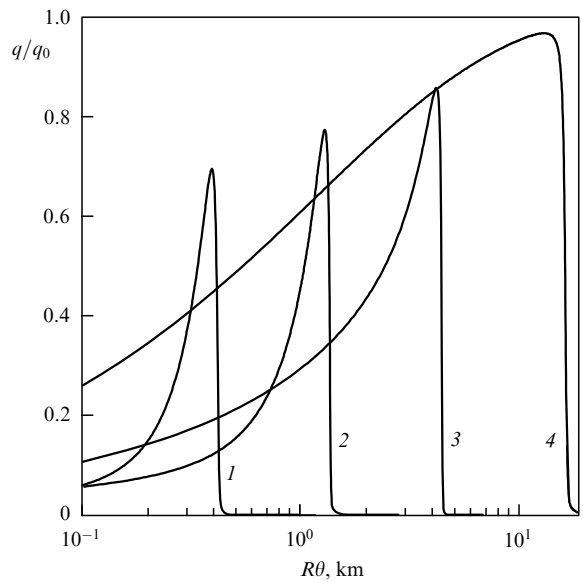

Figure 11. Meridional dependence of the energy flux q_0 emitted from unit surface of the spreading layer: q is the Eddington flux value and $R\theta$ is the linear coordinate measured from the neutron star equator along the meridian. Curves *1–4* correspond to the spreading layer luminosity $L_s/L_{\rm Edd} = 0.01, 0.04, 0.2, 0.8$, respectively. It is seen that, as the boundary layer luminosity rises, the location of bright belts shifts toward the neutron star rotation poles, with their width increasing simultaneously. (Taken from paper [1].)

previously accreted matter — should be decelerated. The wind blowing above a smooth surface may be used as an approximate analog of this problem. At small viscosity, the dependence of the wind velocity on the height is described by the well-known Prandtl–Kármán logarithmic profile (see, for example, Ref. [59]). The solution of the problem of the levitating spreading layer above the neutron star surface was obtained in paper [1] using exactly this approximation. The spreading layer model predictions explain fairly well the observed emission spectra produced in the spreading layer and are in agreement with observations of its time variability.

However, as demonstrated in paper [58], the real situation is more complicated, and the simple solution with thin sole and smooth rotational velocity profile $v_\phi(r)$, in which the velocity v_ϕ decreases to the neutron star rotational velocity due to turbulent viscosity, is possible only with the viscosity coefficient in the Prandtl–Kármán model, which is several hundred times smaller than the commonly accepted value. Similarly, using the α-viscosity model by Shakura and Sunyaev [1] requires the viscosity parameter α taking the values of order $10^{-4} - 10^{-3}$. With the standard parameters, the small turbulent viscosity can only slightly decrease the rotational velocity of the accreting matter, which leads to the appearance of a massive rapidly rotating near-equatorial layer in which the viscous damping of rotation proceeds very slowly.

The azimuthal velocity gradient can generate internal gravity waves in the spreading layer sole, propagating in the flow direction [58]. Nonlinear processes of the wave front turnover link waves propagating in the adjacent layers, and transfer the angular momentum to deep regions of the neutron star, thereby leading to the effective braking of the flow. However, this approach leads to a strong energy release at significant depths corresponding to the surface density $\Sigma > 10^7 - 10^9$ g cm^{-2}. This, in turn, leads to a temperature rise in the deep layers and to stationary helium burning, i.e., to the disappearance of the X-ray burst phenomenon, which evidently contradicts observations. To circumvent this problem, the hypothesis was put forward in paper [58] that a solitary giant gravity wave might be formed at depths corresponding to $\Sigma \sim 10^5 - 10^6$ g cm^{-2}. Such a nonlinear wave can decelerate matter that has fallen out from the levitating layer and reduce the temperature at depths where helium burning takes place, thus opening the possibility for explosive helium burning. Undoubtedly, this hypothesis needs further study; nevertheless, at present, it seems to be more reasonable than the assumption about the anomalously low viscosity coefficients.

Another possible viscosity mechanism that may come into play in the boundary layer was proposed in papers [60, 61]. In that model, the angular momentum is carried by sound waves excited by hydrodynamic instabilities in the shear flow of the boundary layer. Propagating inside and outside the layer and sooner or later decaying, the sound waves transfer the angular momentum to the star and to accretion disk matter located outside the boundary layer, respectively. In this picture, the boundary layer problem becomes much more complicated, since the transfer and dissipation of the angular momentum are no longer local processes determined by the local properties of the flow. Moreover, the sound waves carry both angular momentum and energy, which may cardinally change the energy release in the boundary layer. The efficiency of this braking mechanism, as well as of the mechanism of deceleration due to gravity (surface) waves, is still to be investigated by detailed numerical experiments.

Similar to the spectra of X-ray bursts at luminosities close to the Eddington limit [62], the local spectra of the spreading layer can be described by diluted Planck spectra [36], in which the color and effective temperatures are related as

$$T_{\rm c} = f_{\rm c}\, T_{\rm eff}\,. \tag{15}$$

For the characteristic parameters of the problem studied, the hardness coefficient lies within the range of $f_c \approx 1.6-1.9$. The exact analysis of the radiation transfer in the spreading layer, carried out in paper [36], showed that at sufficiently high accretion rates, $L \geqslant 0.1\,L_{\rm Edd}$, its integral spectrum can also be fairly well described by the one-temperature diluted Planck spectrum. It is important that the color temperature of the spreading layer emission be weakly dependent on its detailed vertical structure and be mostly determined by the neutron star compactness M/R_*. This offers the possibility of estimating the neutron star compactness by measuring the spreading layer spectrum shape (see Section 4). This possibility was successfully realized in papers [24, 36].

To conclude this section, we note that numerical simulations of accretion and the emergence of magneto-rotational instability [63–66] in radiation-dominated accretion disks, which are currently being carried out by many strongest numerical astrophysics groups [67], give hope that numerical modeling of the 3D accretion of matter with high angular momentum onto a weakly magnetized neutron star will be possible in the not distant future. This modeling will allow us not only to test the correctness of approximate semianalytical theoretical models [1, 58, 60], but also to take into consideration the role of magneto-rotational instability in the turbulence formation in the spreading layer and generation of different hydrodynamic and magneto-hydrodynamic instabilities inside it.

4. Observations of boundary layer radiation in galactic X-ray binary systems

Clearly, observations of galactic X-ray binaries could offer the unique opportunity to check the boundary layer theories. However, the similarity of emission spectra from the boundary layer and from the accretion disk complicates the former's measurement. At high accretion rates, $\dot{M} \geqslant 0.05\dot{M}_{\rm Edd}$, both spectra have an approximately Planck form (or represent the sum of several Planck spectra with different temperatures) [1, 2, 36] with somewhat different temperatures and almost the same luminosities (see Fig. 5). Their sum, correspondingly, has a smooth domelike form, on which individual spectral components are indistinguishable (Fig. 12; see also Fig. 5). Moreover, the transition of the accretion flow from the state in which most of the energy is released in the optically thick regime to the optically thin state (corresponding to the transition from the soft to hard spectral state; see Section 2) occurs simultaneously in the accretion disk and boundary layer (see Fig. 6). This complicates the analysis and interpretation of the spectra of X-ray bursters and has led to many ambiguous and contradictory results and conclusions.

The problem was solved in the beginning of the 2000s by utilizing, along with spectral data, information on the X-ray time variability from these sources. As was proposed as early as the 1980s, the characteristics of the time variability can be different for radiation emission from the boundary layer and accretion disk [68]. Further progress became possible after almost 20 years due to the large effective area of detectors of the RXTE observatory and the development of new methods of data analysis. Fourier frequency-resolved spectroscopy was able to show that the spectral-time variability of X-ray flux from accreting neutron stars at frequencies $f \geqslant 1$ Hz at high accretion rate $\dot{M} \geqslant 0.05\dot{M}_{\rm Edd}$ is described by

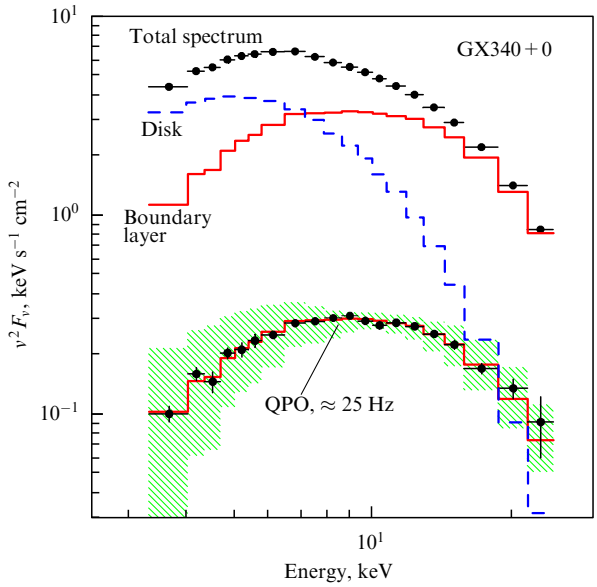

Figure 12. Emission spectra of accretion disk and boundary layer in comparison with the spectrum of the variable component from neutron star GX340+0 observed by RXTE orbital observatory: F_ν is the flux spectral density, and ν is the frequency. The form of the spectrum of the variable component coincides with that of the expected emission spectrum from the boundary layer. Dots with error bars show the total spectrum and the variable component spectrum (QPOs) at a frequency of ≈ 25 Hz. The dashed histogram in the upper part of the figure shows the theoretical spectrum from accretion disk, as described in paper [23]. The solid histogram in the upper part of the figure shows the boundary layer spectrum calculated as the difference between the total observed source spectrum and the theoretical accretion disk spectrum. The solid histogram in the bottom shows the same spectrum normalized to the variable component luminosity. (Takes from paper [23].)

the linear equation [23]

$$S(E,t) = S_0(E) + S_1(E)\,f(t)\,. \tag{16}$$

The analysis of $S_0(E)$ and $S_1(E)$ spectra resulted in the conclusion that the component $S_0(E)$ corresponds to emission from the accretion disk, and the component $S_1(E)\,f(t)$ is from the boundary layer [23, 24] (see Fig. 12). Thus, the X-ray flux variability from accreting neutron stars is due to changes in the luminosity of the boundary layer, whose spectrum remains unchanged. Clearly, $S_1(E)$ stands for the emission spectrum of the boundary layer. It was also demonstrated that the boundary layer spectrum is the same in different sources and changes little when the global accretion rate changes by almost 10 times, in the range $\dot{M} \approx (0.1-0.9)\,\dot{M}_{\rm Edd}$ [23, 24]. With a further increase in the accretion rate $\dot{M} \to \dot{M}_{\rm Edd}$, the boundary layer spectrum approaches a Planck spectrum [23] with temperature $k_{\rm B}T \approx 2.4$ keV for the observer at infinity (Fig. 13).

The independence of the boundary layer emission spectrum from the accretion rate and luminosity gives direct experimental support to the conclusion of the spreading layer theory [1] that the local radiation flux is equal to the Eddington value (see Section 3). The experimentally measured color temperature of the boundary layer emission, $k_{\rm B}T \approx 2.4$ keV, is close to the Eddington temperature on the neutron star surface, given by equation (9). Taking into account the expected hardening factor $T_{\rm c}/T_{\rm eff} \approx 1.7$, it is straightforward to estimate from equation (9) the radius of a neutron star with mass $1.4M_\odot$, at which the color temperature

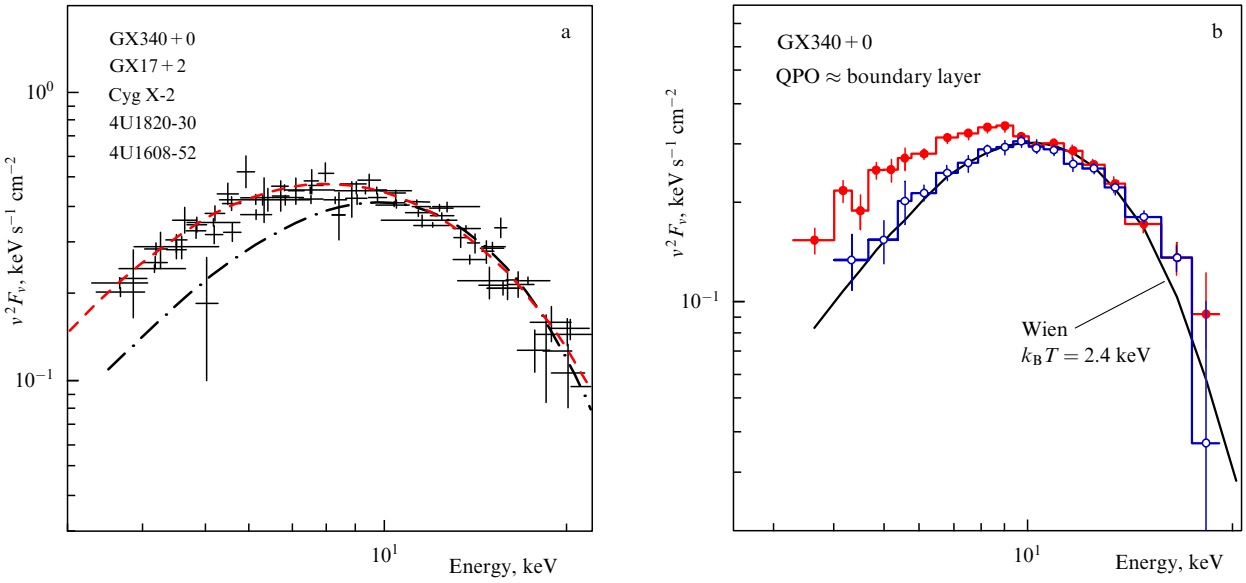

Figure 13. Emission spectra of the boundary layer in several neutron stars, obtained from RXTE observations. (a) Spectra of the variable component for five accreting neutron stars with high luminosities. The figure demonstrates the constancy of the boundary layer spectra in sources wherein luminosities and accretion rates differ by almost 10 times — from $\dot{M} \leqslant 0.1\dot{M}_{\rm Edd}$ to $\dot{M} \sim 0.9\dot{M}_{\rm Edd}$. The spectra are corrected for interstellar absorption. The dashed curve corresponds to a Comptonized emission spectrum with parameters $k_B T_s = 1.5$, $k_B T_e = 3.3$ keV, and $\tau = 5$. The dashed-dotted curve shows a Planck spectrum with temperature $k_B T_{bb} = 2.4$ keV. (Taken from paper [24].) (b) The evolution of the emission spectrum of the variable component in GX 340+0 under changes of accretion rate from $\dot{M} \approx 0.9\dot{M}_{\rm Edd}$ (dark symbols) to $\dot{M} \approx \dot{M}_{\rm Edd}$ (light symbols). The spectra are corrected for interstellar absorption. The solid curve shows a Wien spectrum with temperature $k_B T = 2.4$ keV, which best fits the observed spectrum at $\dot{M} \approx \dot{M}_{\rm Edd}$. At such temperatures, the Wien spectrum for energies $E \geqslant 3$ keV is close to the Planck one. The spectra are normalized to the same radiation flux in the energy range 10–25 keV. (Taken from paper [23].)

of emission with the Eddington radiation flux density is equal to the observed value of $k_B T \approx 2.4$ keV. The radius obtained in this way is $R_* \approx 14$ km. A more detailed analysis [24] with account for the solution of the radiation transfer equation in the spreading layer [34] gives the close values of the neutron star radius and compactness M_*/R_*.

In the spreading layer theory [1], the matter flux through the boundary layer neck is controlled by the matter supply from the extended disk, which is modulated by disk instabilities with long enough characteristic times. Hydrodynamic processes in the levitating spreading layer can enhance this modulation and the variability of the X-ray emission from the bright rings. This explains the significant amplitude of the spreading layer emission variability on time scales much longer than the characteristic times in the boundary layer. It is this variability that was studied by Fourier frequency-resolved spectroscopy, as described above.

However, instabilities should develop in the spreading layer on time scales much shorter (and thus with much higher variability frequencies) than those from an extended accretion disk due to smaller sizes of the former. The velocity of sound in the spreading layer is close to $c_s \sim 0.1c$, and the characteristic sound time in the radial direction, $\tau_{\rm BL} \sim \Delta R_{\rm BL}/c_s$, is a few dozen microseconds. Therefore, in the power spectrum of the X-ray flux fluctuations, an additional component at the characteristic frequencies in the $\sim 5-40$ kHz range should be expected, which is due to turbulence and instabilities of various kinds in the spreading layer. The discovery of such a variability component would provide additional support to the theory and could be a powerful tool for the diagnostics of physical conditions and parameters of turbulence, much like the quasiperiodic and aperiodic variabilities of X-ray binaries at frequencies below ~ 1 kHz have been the probe of the accretion disk, its corona, and (in the case of a neutron star with a strong magnetic field) its interaction with the magnetosphere.

Unfortunately, the sensitivity of the best existing X-ray space telescopes in orbit is insufficient to detect the X-ray flux variability at frequencies $\gtrsim 1$ kHz. The best upper limits on the variability amplitude in this frequency range were obtained by the RXTE orbital observatory, ranging $\sim 5-10\%$ [25]. The prospective orbital missions LOFT (Large Observatory for X-ray Timing) of the European Space Agency and X-ray Microphone (Russia) envision an increase in the effective area of X-ray detectors from $\approx 0.5-1$ m^2, as achieved by the present time on RXTE, to ≈ 10 m^2. This will allow the X-ray timing sensitivity to reach the level of $\sim 10^{-3}-10^{-2}$ (fractional rms) and can result in the discovery of X-ray variability in the kilohertz frequency range. Thus, the possibility will be opened for the experimental probe of turbulence in the spreading layer under physical conditions unavailable in the laboratories on Earth.

5. Conclusion

The impetus for many studies discussed in this review was given by Ya B Zeldovich, who was an outstanding specialist in radiation hydrodynamics and high-temperature phenomena. He drew his pupils' attention to problems of matter accretion onto neutron stars and black holes, which allowed them to obtain many important and interesting results.

Yakov Borisovich was interested in studying the limits of the applicability of the laboratory verified physical laws in unique astrophysical conditions of extremely strong gravitational and magnetic fields and huge radiation energy densities. Problems of accretion, the end stages of the

evolution of massive stars, and processes at the early stages of expansion of the hot Universe inspired him and continue to inspire new generations of young researchers engaged in astrophysics and cosmology. We now know that the methods of observational cosmology and extragalactic astronomy have already led to the discovery of signatures of 'new physics', including dark matter and dark energy, the explanation of which requires fresh ideas and new experiments.

Acknowledgments
One of the authors (R.A.S.) would like to thank N A Inogamov (Landau Institute for Theoretical Physics) for the many fruitful discussions of the topics discussed in the present review.

References

1. Inogamov N A, Sunyaev R A *Astron. Lett.* **25** 269 (1999); *Pis'ma Astron. Zh.* **25**3 23 (1999)
2. Shakura N I, Sunyaev R A *Astron. Astrophys.* **24** 337 (1973)
3. Zel'dovich Ya B, Shakura N I *Sov. Astron.* **13** 175 (1969); *Astron. Zh.* **46** 225 (1969)
4. Kompaneets A S *Sov. Phys. JETP* **4** 730 (1957); *Zh. Eksp. Teor. Fiz.* **31** 876 (1956)
5. Zeldovich Ya B, Sunyaev R A *Astrophys. Space Sci.* **4** 301 (1969)
6. Galloway D *AIP Conf. Proc.* **983** 510 (2008)
7. Shakura N I, Sunyaev R A *Adv. Space Res.* **8** 135 (1988)
8. Kluzniak W, Ph.D. Thesis (Stanford, Calif.: Stanford Univ., 1988)
9. Sibgatullin N R, Sunyaev R A *Astron. Lett.* **24** 774 (1998); *Pis'ma Astron. Zh.* **24** 894 (1998)
10. Grimm H-J, Gilfanov M, Sunyaev R *Astron. Astrophys.* **391** 923 (2002)
11. Liu Q Z, van Paradijs J, van den Heuvel E P J *Astron. Astrophys.* **469** 807 (2007)
12. Liu Q Z, van Paradijs J, van den Heuvel E P J *Astron. Astrophys.* **455** 1165 (2006)
13. Gil'fanov M R *Phys. Usp.* **56** 714 (2013); *Usp. Fiz. Nauk* **183** 752 (2013)
14. Bisnovatyi-Kogan G S, Komberg B V *Sov. Astron. Lett.* **2** 130 (1976); *Pis'ma Astron. Zh.* **2** 338 (1976)
15. Chakrabarty D, Morgan E H *Nature* **394** 346 (1998)
16. Wijnands R, van der Klis M *Nature* **394** 344 (1998)
17. Strohmayer T, Bildsten L, in *Compact Stellar X-ray Sources* (Cambridge Astrophysics Series, No. 39, Eds W Lewin, M van der Klis) (Cambridge, UK: Cambridge Univ. Press, 2006) p. 113
18. Narayan R, Heyl J S *Astrophys. J.* **574** L139 (2002)
19. van der Klis M, in *X-Ray Binaries* (Cambridge Astrophysics Series, No. 26, Eds W H G Lewin, J van Paradijs, E P J van den Heuvel) (Cambridge: Cambridge Univ. Press, 1995) p. 252
20. van der Klis M et al. *Nature* **316** 225 (1985)
21. van der Klis M *Annu. Rev. Astron. Astrophys.* **38** 717 (2000)
22. Stella L, Vietri M *Phys. Rev. Lett.* **82** 17 (1999)
23. Gilfanov M, Revnivtsev M, Molkov S *Astron. Astrophys.* **410** 217 (2003)
24. Revnivtsev M G, Gilfanov M R *Astron. Astrophys.* **453** 253 (2006)
25. Sunyaev R, Revnivtsev M *Astron. Astrophys.* **358** 617 (2000)
26. Giacconi R et al. *Astrophys. J.* **167** L67 (1971)
27. Gnedin Yu N, Sunyaev R A *Astron. Astrophys.* **25** 233 (1973)
28. Basko M M, Sunyaev R A *Astron. Astrophys.* **42** 311 (1975)
29. Basko M M, Sunyaev R A *Sov. Astron.* **20** 537 (1976); *Astron. Zh.* **53** 950 (1976)
30. Lipunov V M *Astrophysics of Neutron Stars* (Berlin: Springer-Verlag, 1992); Translated from Russian: *Astrofizika Neitronnykh Zvezd* (Moscow: Nauka, 1987)
31. Ghosh P *Rotation and Accretion Powered Pulsars* (Hackensack, N.J.: World Scientific, 2007)
32. Syunyaev R A, Shakura N I *Sov. Astron. Lett.* **12** 117 (1986); *Pis'ma Astron. Zh.* **12** 286 (1986)
33. Lorenz C P, Ravenhall D G, Pethick C J *Phys. Rev. Lett.* **70** 379 (1993)
34. Sibgatullin N R, Sunyaev R A *Astron. Lett.* **26** 699 (2000); *Pis'ma Astron. Zh.* **26** 813 (2000)
35. Kluzniak W, Wilson J R *Astrophys. J.* **372** L87 (1991)
36. Suleimanov V, Poutanen J *Mon. Not. R. Astron. Soc.* **369** 2036 (2006)
37. Özel F, Baym G, Güver T *Phys. Rev. D* **82** 101301(R) (2010)
38. Shimura T, Takahara F *Astrophys. J.* **445** 780 (1995)
39. Sunyaev R A, Titarchuk L G *Astron. Astrophys.* **86** 121 (1980)
40. Sunyaev R A, Titarchuk L, in *Proc. of the 23rd ESLAB Symp. on Two Topics in X-Ray Astronomy, Bologna, Italy, 13 – 20 September 1989* Vol. 1 (ESA SP, No. 296, Eds J Hunt, B Battrick) (Paris: European Space Agency, 1989) p. 627
41. Gilfanov M, Churazov E, Revnivtsev M *Mon. Not. R. Astron. Soc.* **316** 923 (2000)
42. Gilfanov M *Lecture Notes Phys.* **794** 17 (2010)
43. Churazov E, Gilfanov M, Revnivtsev M *Mon. Not. R. Astron. Soc.* **321** 759 (2001)
44. Orosz J A et al. *Astrophys. J.* **742** 84 (2011)
45. Shakura N I, Sunyaev R A *Mon. Not. R. Astron. Soc.* **175** 613 (1976)
46. Narayan R, Yi I *Astrophys. J.* **428** L13 (1994)
47. Garcia M R et al. *Astrophys. J.* **553** L47 (2001)
48. Levich E V, Syunyaev R A *Sov. Astron.* **15** 363 (1971); *Astron. Zh.* **48** 461 (1971)
49. Abramowicz M A et al. *Astrophys. J.* **332** 646 (1988)
50. Paczyńsky B, Wiita P J *Astron. Astrophys.* **88** 23 (1980)
51. Pringle J E *Mon. Not. R. Astron. Soc.* **178** 195 (1977)
52. Pringle J E, Savonije G J *Mon. Not. R. Astron. Soc.* **187** 777 (1979)
53. Tylenda R *Acta Astron.* **31** 267 (1981)
54. Meyer F, Meyer-Hofmeister E *Astron. Astrophys.* **221** 36 (1989)
55. Bisnovatyi-Kogan G S *Mon. Not. R. Astron. Soc.* **269** 557 (1994)
56. Popham R, Narayan R *Astrophys. J.* **442** 337 (1995)
57. Popham R, Sunyaev R *Astrophys. J.* **547** 355 (2001)
58. Inogamov N A, Sunyaev R A *Astron. Lett.* **36** 848 (2010); *Pis'ma Astron. Zh.* **36** 896 (2010)
59. Landau L D, Lifshitz E M *Fluid Mechanics* (Oxford: Pergamon Press, 1987); *Gidrodinamika* (Moscow: Nauka, 1986)
60. Belyaev M A, Rafikov R R *Astrophys. J.* **752** 115 (2012)
61. Belyaev M A, Rafikov R R, Stone J M *Astrophys. J.* **770** 67 (2013)
62. Lapidus I I, Syunyaev R A, Titarchuk L G *Sov. Astron. Lett.* **12** 383 (1986); *Pis'ma Astron. Zh.* **12** 918 (1986)
63. Velikhov E P *Sov. Phys. JETP* **9** 995 (1959); *Zh. Eksp. Teor. Fiz.* **36** 1398 (1959)
64. Chandrasekhar S *Proc. Natl. Acad. Sci. USA* **46** 253 (1960)
65. Balbus S A, Hawley J F *Astrophys. J.* **376** 214 (1991)
66. Hawley J F, Balbus S A *Astrophys. J.* **376** 223 (1991)
67. Jiang Y-F, Stone J M, Davis S W *Astrophys. J.* **778** 65 (2013)
68. Mitsuda K et al. *Publ. Astron. Soc. Jpn.* **36** 741 (1984)